Current Biology, Volume *22*

Supplemental Information

Noise and Correlations

in Parallel Perceptual Decision Making

Thomas U. Otto and Pascal Mamassian

Supplemental Inventory

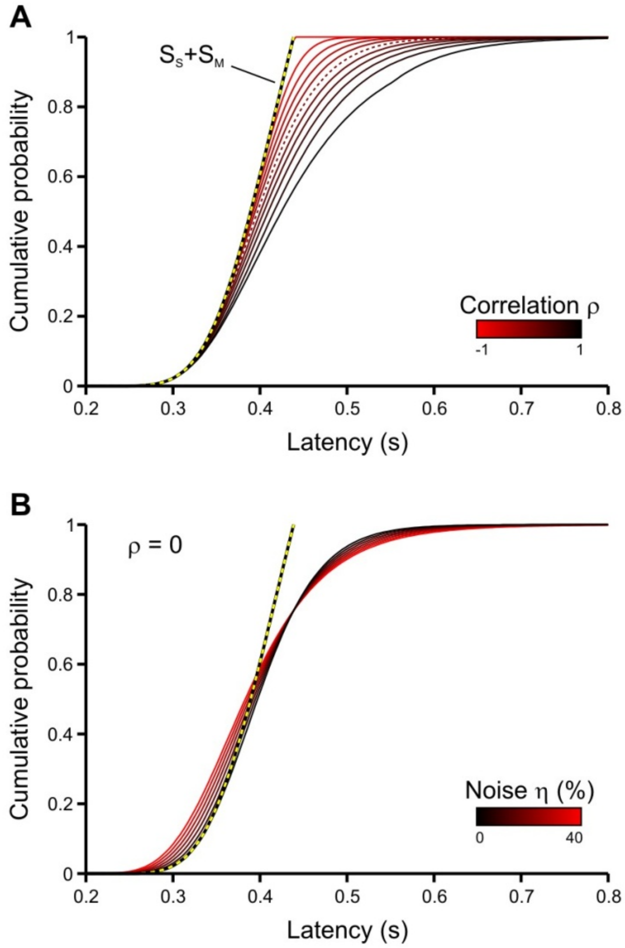

Figure S1. Predictions for Condition R_{MS} Based on Probability Summation and the Corresponding Single Conditions S_M and S_S

The framework is introduced in Figure 1, main text.

(A) We systematically varied the correlation coefficient ρ. The expected speed-up of latencies is largest assuming a maximal negative correlation. Critically, Boole's inequality (see S_M+S_S) provides an upper bound that is not violated. The prediction assuming statistical independence is highlighted by a broken line (ρ=0; see Equation 1, main text).

(B) We extended the probability summation model by allowing for additional noise η when signals are processed simultaneously. With additional noise (in % relative to single conditions), violations of Boole's inequality occur for fastest latencies similar to empirical distributions (see Figure 2B, main text). Critically, the speed-up of fastest responses comes at the cost of a slow-down of slowest responses. Hence, latencies are overall more variable.

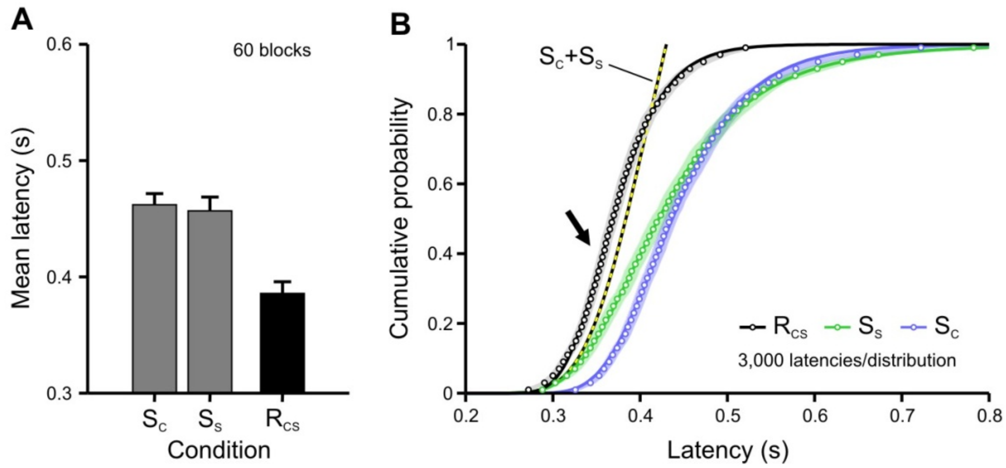

Figure S2. The Redundant Signal Effect with Color and Sound Signals

Results are analogous to the experiment with motion and sound signals (see Figure 2, main text).

(A) Mean latencies in the redundant condition R_{CS} were faster compared to single conditions S_C and S_S (mean and SEM of 60 blocks with 50 latencies each).

(B) Cumulative distributions (circles and shaded areas indicate group quantiles with SEM; best-fitting recinormal distributions are shown as solid lines). The shift of the R_{CS} distribution to the left corresponds to the speed-up of mean latencies (see A). Numerous quantiles in condition R_{CS} exceeded the theoretical bound provided by the sum of distributions in conditions S_C and S_S (arrow).

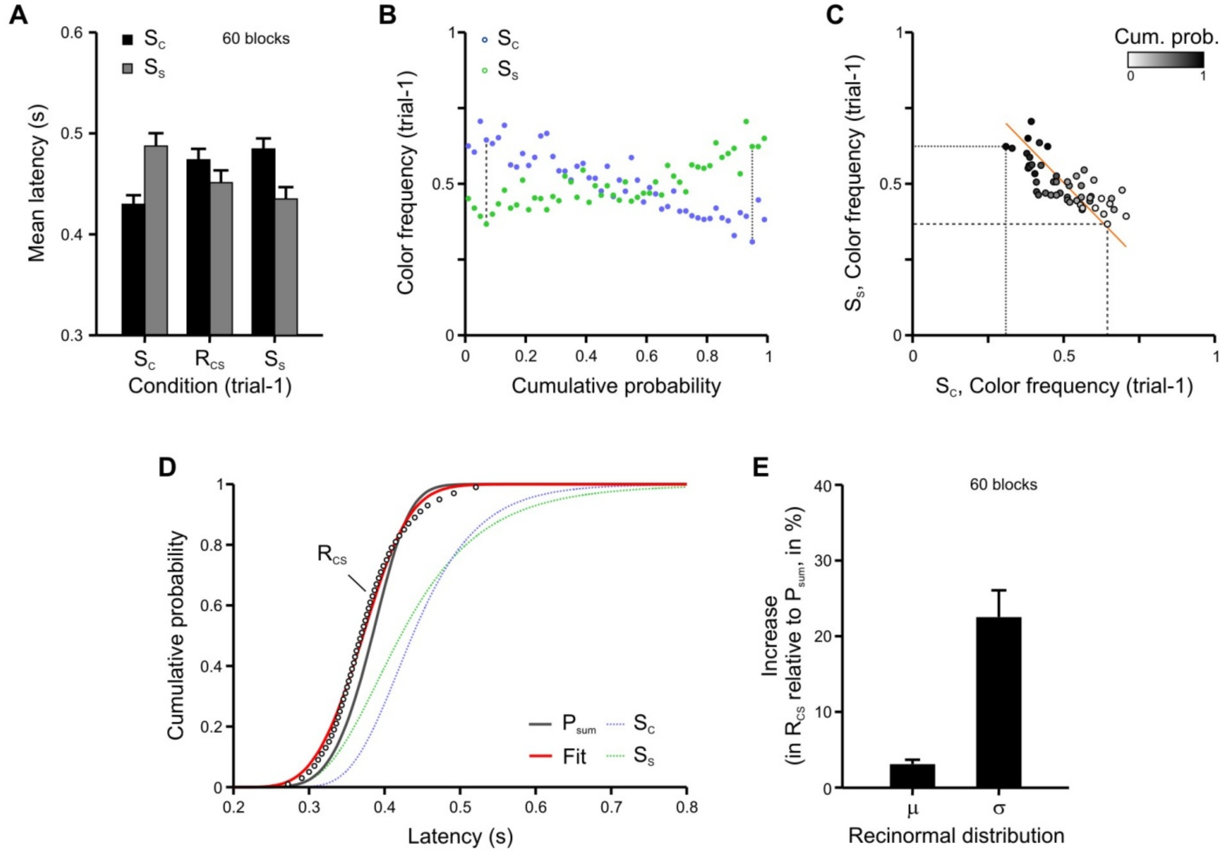

Figure S3. Interactions with Color and Sound Signals

Results are analogous to the experiment with motion and sound signals (see Figure 3, main text).

(A) Mean latencies depended on the condition that was presented on the previous trial.

(B) For each group quantile of conditions S_C and S_S (see Figure S2), we determined the relative frequency of color signals presented on the previous trial. A value close to one (zero) indicates that most responses summarized by a quantile were preceded by a color (sound) signal.

(C) The analysis of color frequencies showed a negative correlation between latencies in single conditions (Pearson's linear correlation coefficient, ρ_H=-0.76, p<0.0001; numerical values of ρ_H across experiments were by chance identical).

(D) Based on the single conditions, we fitted the probability summation model with the correlation coefficient ρ as a free parameter to the latency distribution in condition R_{CS} ("P_{sum}"). The empirical distribution deviated from P_{sum} in that most quantiles were faster except for the slowest quantiles that were slower than predicted (see also E). The extended model with the correlation coefficient ρ and the additional noise η as free parameters provided a reasonable "Fit" to the empirical distribution (best-fitting parameters are summarized in Table S2).

(E) We tested for deviations from P_{sum} using the parameters of recinormal distributions fitted separately to the empirical and predicted quantiles of each block. While the mean μ was slightly elevated (one-sample t-test, p<0.0001), the standard deviation σ was largely increased (one-sample t-test, p<0.0001).

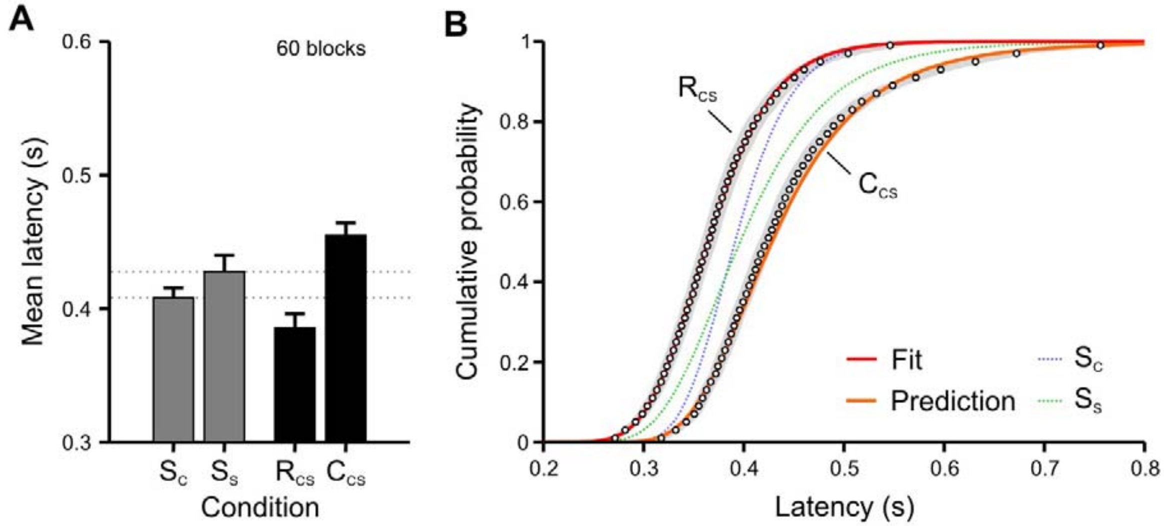

Figure S4. Predictions with Color and Sound Signals

Results are analogous to the experiment with motion and sound signals (see Figure 4, main text). We presented conditions in separate blocks of trials (S_C, S_S, and R_{MS}). We included also a new condition in which targets were defined by a conjunction of color and sound signals (C_{CS}).

(A) Mean latencies. While responses in condition R_{CS} were sped-up, responses in condition C_{CS} were slowed-down. Mean and SEM of 60 blocks.

(B) Cumulative distributions. The extended model with the correlation coefficient ρ and the additional noise η as free parameters provided an excellent "Fit" for condition R_{CS} (the best-fitting parameters are summarized in Table S2). Using identical parameters, the model nicely predicted the distribution in condition C_{CS}. Each distribution is based on 3,000 responses.

Table S1. Best-Fitting Recinormal Distributions

Experiment	Condition	μ (s^{-1})	σ (s^{-1})	RMSE
Random	S_M	2.222	0.364	0.011
	S_S	2.354	0.482	0.003
	R_{MS}	2.640	0.355	0.005
	S_C	2.288	0.355	0.008
	S_S	2.373	0.481	0.003
	R_{CS}	2.710	0.341	0.008
Block by block	S_C	2.555	0.290	0.014
	S_M	2.396	0.329	0.010
	S_S	2.522	0.433	0.004
	R_{MS}	2.678	0.389	0.007
	R_{CS}	2.747	0.384	0.006
	C_{MS}	2.199	0.364	0.013
	C_{CS}	2.355	0.375	0.015

Table S2. Best-Fitting Model Parameters

Experiment	Condition	Model*	ρ	η (s^{-1})	RMSE
Random	R_{MS}	C	-0.70	-	0.067
		N	-	0.137 (~32%)**	0.058
		C+N***	-0.59	0.097 (~23%)**	0.019
	R_{CS}	C	-0.82	-	0.094
		N	-	0.182 (~43%)**	0.074
		C+N***	-0.72	0.130 (~31%)**	0.022
Block by block	R_{MS}	C	0.10	-	0.030
		N	-	0.042 (~11%)**	0.021
		C+N***	0.21	0.059 (~15%)**	0.006
	R_{CS}	C	0.13	-	0.045
		N	-	0.059 (~16%)**	0.029
		C+N***	0.29	0.083 (~23%)**	0.005
	C_{MS}	Prediction	from R_{MS}	from R_{MS}	0.034
		C+N	-0.04	0.074 (~19%)**	0.010
	C_{CS}	Prediction	from R_{CS}	from R_{CS}	0.022
		C+N	0.37	0.055 (~15%)**	0.010

*Correlation only (C), Noise only (N), Correlated and noise (C+N).
**Compared to the average standard deviation in corresponding single conditions (see Table S1).
***The extended model provided a significantly better fit compared to both restricted models (extra sum-of-squares F test, p<0.0001 in all cases).

Supplemental Experimental Procedures

Experimental Setup
Participants were tested individually in an isolated experimental room. Auditory stimuli were presented to both ears simultaneously through Sennheiser HD-280 Pro headphones. Visual stimuli were presented on a Sony GDM-C520 CRT monitor (100 Hz refresh rate). Viewing distance was 60 cm supported by a chin rest. A computer running MATLAB (The MathWorks) equipped with standard toolboxes [48, 49] controlled stimulus presentation and the collection of responses via the keyboard.

Auditory Stimulation
Auditory background noise was continuously presented in all conditions. Noise consisted of Gaussian noise (i.e., a sequence of normally distributed random numbers at a sample rate of 44.1 kHz) which was filtered so that most of the power was between 262-330 Hz. The presentation level of the background noise was 53 dB(A) as measured using an artificial ear adaptor. As sound signals, we presented 294 Hz tones (the note D) that were embedded in the noise. Tones were presented for 500 ms including sinusoidal ramp on- (10 ms) and offsets (100 ms). The presentation level of the tones was 53 dB(A).

Visual Stimulation
Visual background noise was continuously presented in all conditions. The noise was composed of 200 white dots (2x2 pixels) on a dark grey background. Dots moved linearly in random directions with a speed of 1 deg/s. Dots were restricted to the area of a notional annulus with an inner/outer diameter of 0.5/5.0 deg around central fixation. On each refresh, dots falling outside the area and some of the remaining dots (with a probability of 1%) were randomly re-located within the area of the notional annulus. As visual signals, we changed the motion or the color of some dots. With motion signals, 50% of the dots changed from random motion to coherent rotation around fixation (0.14 cps). With color signals, 30% of the dots turned yellow. In both cases, signals were presented for 500 ms and dots returned to white and random motion, respectively.

Task and Procedures
Participants were instructed to detect target signals by pressing a button. We asked participants to respond as fast as possible, but to avoid false alarms and missed targets. We employed a partially self-paced, continuous stimulation paradigm. Auditory and visual background noise was presented throughout a block. After a random interval of 1500-3500 ms (uniformly distributed), a target was presented. At the time of a response, a new random interval preceding the next target was triggered.

We considered responses with latencies within 100-1500 ms after signal onset as valid. Responses falling outside this range were false alarms (~2% across all conditions) and missed targets (<1%), respectively. After an error, a feedback-screen, which indicated the error, interrupted the continuous stimulation for 1500 ms before a new random interval preceding the next target was triggered.

In Experiment 1, conditions were randomly interleaved within a block. This included two single conditions (only the auditory or only the visual signal was presented) and one redundant condition (both signals were presented simultaneously; see Figure 1A,B). For each condition, we collected 55 valid responses per block. A block lasted about 9 min and was interrupted twice by a pause-screen to offer participants a short rest.

In Experiment 2a, we tested the same three conditions as in Experiment 1 but we presented each condition in a separate block of trials. In Experiment 2b, targets were defined by a conjunction of two signals (both the auditory and the visual signal were presented simultaneously as in the redundant conditions; Figure 1F). Critically, the random interval of 1500-5000 ms preceding a target could contain non-target signals (only the auditory or only the visual signal was presented). Participants had to withhold a response on presentation of single signals. A block contained about twice as many non-targets than targets. In each block of Experiment 2, we collected 55 valid responses. A block lasted about 3-4 min.

Participants were familiarized with all conditions in a short practice session before the experiment proper (about 5-10 min). Participants then performed 4 sessions lasting about 1 h each. To reduce fatigue effects, participants performed not more than 2 sessions on a day. Within a session, we presented a block of each condition once. Each block was introduced by a start-screen indicating the next condition by an animation of possible targets and non-targets. Participants initiated blocks by a button press. At the end of a block, the start-screen for the next block appeared. We encouraged participants to use these occasions to take a rest. The order of conditions/blocks was randomized across observers and sessions.

Latency Analysis

All analysis and modeling was performed using MATLAB (The MathWorks). We used a reciprocal scale (1/latency) for the analysis of response latencies (except for the computation of simple mean latencies). Mean latencies of one condition measured with one participant but in different sessions could differ by several 10s of ms, which is possibly related to learning or fatigue that might occur across sessions or to other general effects. To avoid that such differences affect the shape (and particularly the variance) of the estimated group latency distributions [30], we considered each block as an independent sample instead of pooling latencies across sessions. To reduce the impact of anticipatory responses and lapses of attention, we performed an outlier correction on the basis of the 55 valid responses of each block and condition. We rejected trials with latencies deviating by more than 3 standard deviations from the mean on the reciprocal scale (about 0.8% of the trials). Then, to obtain equally sized data blocks, we selected the latest 50 trials of each block/condition (the first few trials were considered as training and not further analyzed). In total, we collected 60 equally sized data blocks summing up to 3,000 latencies per condition (39,000 responses were collected for the whole study).

To obtain cumulative group distributions, we rank ordered the latencies of each block and averaged response latencies of each rank on the reciprocal scale (Vincent averaging [30]; e.g., the latency of the fastest group quantile is computed by the average latency of the fastest response within each block, and so forth for the remaining ranks). With this method, we obtained 50 group quantiles that were based on 60 responses each. To obtain continuous distribution functions, we fitted recinormal distributions (i.e., normal distributions on the reciprocal scale) to the group quantiles of each condition by minimizing the root mean squared error (RMSE; using the “fminsearch” routine of MATLAB). Estimates of the mean (μ) and the standard deviation (σ) of the group distribution were virtually identical to the averaged estimates of the individual blocks.

Trial History Analysis

For each response in Experiment 1, we recorded the condition that was presented on the previous trial. For the 60 responses of a given quantile, we computed the relative frequency of signals that were presented on the previous trial. For example, with motion and sound signals, the “motion frequency” is given by the number of motion signals divided by the total number of sound and motion signals on the previous trial. Note that the total number of signals could be larger than 60 because two signals were presented in redundant conditions.

Model

We predicted the latency distribution with redundant signals based on probability summation. The exact distribution is given by the minimum function of the latency distributions in the single conditions, which can be estimated using the maximum function of the corresponding drift rate distributions (Figure 1C-E). For two Gaussian random variables the exact maximum function is known [34]. Let (D_A, D_V) denote a bivariate Gaussian random vector with means (μ_A, μ_V), variances (σ_A^2, σ_V^2) and correlation coefficient ρ. The probability density function of the maximum distribution is given by $f(x) = f_1(-x) + f_2(-x)$, with

$$f_1(x) = \frac{1}{\sigma_A}\phi\left(\frac{x+\mu_A}{\sigma_A}\right) \times \Phi\left(\frac{\rho(x+\mu_A)}{\sigma_A\sqrt{1-\rho^2}} - \frac{x+\mu_V}{\sigma_V\sqrt{1-\rho^2}}\right) \qquad \text{(Equation S1)}$$

and

$$f_2(x) = \frac{1}{\sigma_V}\phi\left(\frac{x+\mu_V}{\sigma_V}\right) \times \Phi\left(\frac{\rho(x+\mu_V)}{\sigma_V\sqrt{1-\rho^2}} - \frac{x+\mu_A}{\sigma_A\sqrt{1-\rho^2}}\right) \qquad \text{(Equation S2)}$$

where $\phi(\cdot)$ and $\Phi(\cdot)$ are the probability density function and the cumulative distribution function of the standard normal distribution, respectively. Thus, with the drift rates $D_A \sim N(\mu_A, \sigma_A^2)$ and $D_V \sim N(\mu_V, \sigma_V^2)$ as determined in the single conditions, the probability summation model had only one degree of freedom, i.e., the correlation coefficient ρ.

To model the noise interaction in redundant conditions, the interaction noise η is added to the standard deviation of the two drift rates as determined in the corresponding single conditions. Thus, if drift rates $D_A \sim N(\mu_A, \sigma_A^2)$ and $D_V \sim N(\mu_V, \sigma_V^2)$ were determined in single conditions with auditory and visual signals, we used the adapted drift rates $D_A' \sim N(\mu_A, (\sigma_A + \eta)^2)$ and $D_V' \sim N(\mu_V, (\sigma_V + \eta)^2)$ for model predictions of the redundant condition. Model predictions were then computed analogously to predictions based on probability summation using the adapted drift rates (see Equations S1 and S2). Thus, the extended model had two degrees of freedom, the correlation coefficient ρ and the additional noise η. We fitted the model to empirical distributions by minimizing the RMSE. Model fitting and prediction of latency distributions with conjunction signals was performed analogously using the minimum instead of the maximum function [34] of the corresponding drift rates.

Supplemental References

48. Brainard, D.H. (1997). The psychophysics toolbox. Spat. Vis. 10, 433-436.

49. Pelli, D.G. (1997). The VideoToolbox software for visual psychophysics: Transforming numbers into movies. Spat. Vis. 10, 437-442.